Journal of Hydrology (2008) **357**, 255–269

available at www.sciencedirect.com

ScienceDirect

journal homepage: www.elsevier.com/locate/jhydrol

Investigating the roles of climate seasonality and landscape characteristics on mean annual and monthly water balances

Yoshiyuki Yokoo [a,*], Murugesu Sivapalan [a,1], Taikan Oki [b]

[a] *Centre for Water Research, University of Western Australia, 35 Stirling Highway, Crawley, Western Australia 6009, Australia*
[b] *Institute of Industrial Science, The University of Tokyo, 4-6-1 Komaba, Meguro, Tokyo 153-8505, Japan*

Received 21 June 2007; received in revised form 2 May 2008; accepted 7 May 2008

KEYWORDS
Climate;
Soil;
Topography;
Seasonality;
Water balance;
Dryness

Summary This paper explores the effects of seasonal variability of climatic inputs on mean annual and monthly water balances and the roles of climate, soil properties and topography in modulating these impacts. The analyses are carried out with the use of a theoretically derived and physically-based water balance model, which includes simple sub-models for evapotranspiration, infiltration, surface runoff by both infiltration excess and saturation excess, and subsurface runoff. Numerical experiments for different watershed conditions showed (1) the effects of seasonality are most important when the seasonal variabilities of precipitation and potential evapotranspiration are out of phase, and in arid climates, (2) the seasonality effects are found to be high in basins with fine grained soils and flat topographies, in which case surface runoff dominates, and also high in basins with coarse grained soils and steep topographies, where subsurface runoff dominates. Indeed, there appears to be a critical combination of soil type and gradient at which a switch from subsurface to surface runoff dominance takes place. As one moves from well drained to poorly drained catchments, the amplitude of the resulting seasonal fluctuations initially decreases and beyond some threshold value of drainability it might increase again due to the switch from subsurface to surface runoff dominance. The study also highlighted the important role of the unsaturated zone storage, the effects of soil permeability and their interactions with topographic slope, in determining both annual and seasonal water balances. The results of the study are summarized in terms of soil type

* Corresponding author. Present address: ''Wisdom of Water'' (Suntory) Corporate Sponsored Research Program, Organization for Interdisciplinary Research Projects, The University of Tokyo, 4-6-1 Komaba, Meguro, Tokyo 153-8505, Japan. Tel.: +81 3 5452 6382; fax: +81 3 5452 6383.
E-mail addresses: yokoo@iis.u-tokyo.ac.jp (Y. Yokoo), sivapala@uiuc.edu (M. Sivapalan).
[1] Present address: Departments of Geography and Civil and Environmental Engineering, University of Illinois at Urbana-Champaign, 220 Davenport Hall, 607 S. Mathews Avenue, Urbana IL 61801, USA.

0022-1694/$ - see front matter
doi:10.1016/j.jhydrol.2008.05.010

and three dimensionless numbers: climatic dryness index, storage capacity index and drainability index.

Introduction

The partitioning of rainfall into its various components and the role of the climatic, soil, topographic and vegetation properties in this partitioning are fundamental issues in hydrologic science. Understanding of the rainfall partitioning becomes most useful when hydrologists are asked to make predictions of the responses of ungauged basins from the knowledge of climate and basin properties alone, without the benefit of calibration (Sivapalan et al., 2003). The research presented in this paper has been motivated by the general scientific question: what are the relative controls of climatic, soil, vegetation and topographic conditions on the rainfall partitioning? Eagleson (1978a,b) and Reggiani et al. (2000) tried to address this question at many different levels, but did not explicitly consider the effect of climatic seasonality, especially when the contrast between rainy and dry seasons is strong. Milly (1994a,b) used a conceptual (bucket) model to investigate the effects of climatic seasonality in terms of interactions of seasonal fluctuations with the storage capacity of the soil; however, the roles of topography and catchment's drainage properties (e.g., permeability of the soils) were not explicitly considered. Woods (2003) extended the analytical approach of Milly (1994a,b) to also include water storage and release by the plant canopy and saturated soil zone. In a recent study Potter et al. (2005) investigated the effects of climate seasonality on mean annual water balance in Australian catchments and concluded that both catchment-scale soil moisture capacity and infiltration capacity are important determinants of annual water balance. Thus the competing effects of climate fluctuations and catchment storage capacity or infiltration capacity have been studied extensively in previous studies of Milly (1994a,b), Woods (2003) and Potter et al. (2005). The effects of topography and subsurface drainage become important at intra-annual and inter-annual timescales and their impacts on both annual and monthly water balances have not been explored sufficiently in these previous studies. Salvucci and Entekhabi (1995) extended the mathematical formulations of Eagleson's (1978a,b) work to include lateral flow processes in hillslopes. However, their work did not extend to the study of the effects of climate seasonality.

The main objective of this paper is to investigate the effects of seasonal climatic variability on annual and monthly water balances through its interaction with a few key catchment physiographic characteristics, including topography, in this way extending the work of Milly (1994a,b), Woods (2003) and Salvucci and Entekhabi (1995). To achieve this objective we employ the model of Reggiani et al. (2000) and will introduce seasonal variation of climate into the input data that will drive the model. We have designed our explorations of the process controls on monthly and annual water balances in such a way as to enable comparisons with the previous results of Eagleson (1978a,b), Milly (1994a,b), Woods (2003) and Salvucci and Entekhabi (1995) for the effects of seasonality on annual water balance. On the other hand, this paper is restricted to the water balance in rain driven systems only, and does not address snowpack or glacier or wetland dynamics. The ultimate objective is to gain insightful understanding of the climatic and landscape controls on annual and monthly water balances in rainfall driven catchments, sufficient to make meaningful comparisons of catchment responses in different parts of the world, and to guide future observations and approaches to data analysis. Towards this end, the results of these simulations will be used to guide the development of dimensionless similarity parameters that could characterize the dominant hydrological processes in a given basin and embrace the net effects of the interactions of climatic properties and landscape characteristics.

Water balance model

Assumptions and model limitations

For simplicity, this study employs the lumped, physically-based water balance model developed by Reggiani et al. (2000) as shown schematically in Fig. 1. Although the representative elementary watershed (REW) approach adopted by Reggiani et al. (1998, 1999, 2000) is amenable to distributed modelling through the use of multiple REWs, in this study we explore the response of a single REW only. Possible lateral exchanges of water among different REWs are ignored and are not discussed in our results. As in the case of Reggiani et al. (1998, 1999, 2000), our model does not

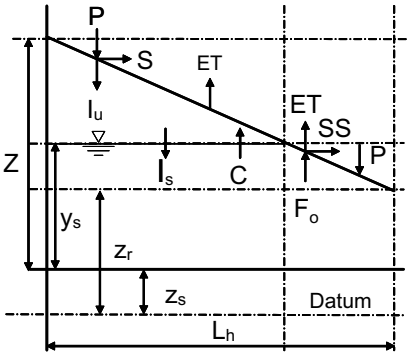

Figure 1 Conceptual drawing of Reggiani et al.'s (2000) REW scale water balance model. *P*: Precipitation, *ET*: Evapotranspiration, *PET*: Potential evapotranspiration, *S*: Surface runoff, *SS*: Subsurface runoff, I_u: Infiltration from the ground surface to the unsaturated zone, I_s: Infiltration from the unsaturated zone to the saturated zone, *C*: Capillary rise, F_o: Outflow from saturated zone, z_r: Average elevation of channel bed with respect to datum, z_s: Average elevation of the bottom surface of the REW with respect to datum, y_s: Average thickness of saturated zone, L_h: Averaged horizontal length of one side of a REW.

capture root water uptake processes in sufficient detail, and only uses a simplified treatment of evapotranspiration. In addition, the constitutive relationships of the governing equations and their parameter settings, which control the partitioning of precipitation into evapotranspiration, surface runoff and subsurface runoff, still require further improvements. Hence evapotranspiration estimates predicted by our model may not reflect reality sufficiently well and may be too crude compared to other more sophisticated models. Our contention is that this simplified treatment is sufficient for the purpose at hand, namely, to explore the first order effects of climate seasonality on annual and monthly water balances.

Governing equations

The governing (coupled mass and momentum balance) equations used in this study for the unsaturated and saturated zones of a typical REW are slight adaptations of the equations given in Appendix A of Reggiani et al. (2000), who derived these equations rigorously and from the first principles at the scale of a REW. Note that Reggiani et al. (2000) introduced many assumptions for the closure of the equations, which should influence the applicability and results of the model. A slight adaptation is made for the evapotranspiration component in the mass balance equation for the unsaturated zone; this is the underlined part in Eq. (1) below. The momentum balance equation for the unsaturated zone in Eq. (2) and the mass balance equation for the saturated zone presented in Eq. (3) are not different from Reggiani et al. (2000).

$$\underbrace{\rho\varepsilon\frac{d}{dt}(s_u y_u \omega_u)}_{\text{Change in unsaturated storage}} = \underbrace{\min\left\{\rho P\omega_u, \frac{\rho K_s \omega_u}{\Lambda_u}\left[\frac{1}{2}y_u - \psi_u\right]\right\}\cdot\delta[0,t_r]}_{\text{Infiltration}} + \underbrace{\rho\varepsilon\omega_u v_u}_{\text{Percolation or capillary rise}} \underbrace{-\rho\omega_u\frac{1}{R}(\tanh 5s_u)(1.0+R^{-5})^{-(1/5)}PET\cdot\delta[t_r,t_m]}_{\text{Evapotranspiration}} \quad (1)$$

$$\underbrace{-\varepsilon\rho g s_u y_u \omega_u}_{\text{Gravitational force}} + \underbrace{\varepsilon\rho g s_u \omega_u\left[\frac{1}{2}y_u - \psi_u\right]}_{\text{Force acting on the water across the land surface}} = \underbrace{K^{-1}\varepsilon\rho g y_u \omega_u v_u}_{\text{Resistance force}} \quad (2)$$

$$\underbrace{\rho\varepsilon\frac{d}{dt}(y_s\omega_s)}_{\text{Change in the saturated storage}} = -\underbrace{\rho\varepsilon\omega_u v_u}_{\text{Percolation or capillary rise}} \underbrace{-\frac{\rho K_s\omega_o}{\cos(\gamma_o)\Lambda_s}\frac{1}{2}(y_s - z_r + z_s)}_{\text{Outflow across seepage faces}} \quad (3)$$

The function $\delta[0, t_r]$ (resp. $\delta\,[t_r, t_m]$) in Eq. (1) is equal to 1 if the time t in a meteorological period, which consists of a storm period and an inter-storm period, falls between 0 (resp. t_r) and t_r (resp. t_m), and is zero otherwise. The variables s_u, y_u, ω_u, Λ_u, ψ_u, v_u, K, P, and PET are, respectively, saturation degree in the unsaturated zone, average thickness of unsaturated zone, unsaturated surface area fraction, characteristic length scale for infiltration, pressure head in the unsaturated zone, upward velocity in the unsaturated zone, unsaturated hydraulics conductivity, precipitation, and seasonally-varying potential evapotranspiration. The variables y_s, ω_s, ω_o, γ_o, and Λ_s are, respectively, average thickness of the saturated zone, area fraction of saturated zone, saturated surface fraction, slope angle of the overland flow plane with respect to horizontal, and typical length scale for seepage outflow. The definitions of the other variables used in these equations are summarized in Table 1 as well as in the appendix of Reggiani et al. (2000). These equations contain 7 unknowns, and therefore 4 additional closure equations are required. Most of those are trivial geometric facts, but the parameterization of seepage area fraction ω_o is a non-trivial one requiring further assumptions, as outlined below:

$$\omega_o = \frac{y_s - z_r + z_s}{Z - z_r + z_s} \quad (4)$$

$$\dot{\omega}_o = -\dot{\omega}_u \quad (5)$$

In Eq. (4), Z is the average thickness of the subsurface zone, z_r is channel bed elevation with respect to a datum, z_s is the average elevation of the bottom surface of the REW with respect to the datum, y_s is the average thickness of the subsurface zone along the vertical, and ω_u is the area fraction of the unsaturated zone.

Since we are only concerned with long-term (annual and monthly) water balances, those short term landscape processes that do not have a bearing on longer term water balances are removed from explicit consideration, as in Reggiani et al. (2000), such as the detailed routing response of overland flow and channel flow.

Although the original model of Reggiani et al. (2000) assumed actual evapotranspiration to be linearly proportional to the saturation degree in the unsaturated zone, s_u, we modified it slightly, as shown in the underlined part in Eq. (1) above. The application of the original model for a steep watershed (slope gradient $G = 0.004$ as defined later) covered with 8 m deep silty loam and experiencing stationary climatic conditions (i.e. without seasonality and constant ''storminess index'', i.e., ratio of storm period over inter-storm period, set at $T = 5.0$), as in Reggiani et al. (2000), tended to produce annual evapotranspiration values different from empirically based estimates such as given by Budyko (1974), Choudhury (1999), Ol'dekop (1911), Pike (1964), Schreiber (1904), Turc (1954) and Zhang et al. (2001) as shown in Fig. 2(b). Fig. 2(b) also shows an example of annual evapotranspiration for a particular condition by the original model in Reggiani et al. (2000) that can change with the choices of climatic and landscape properties as shown in Fig. 2(c) where the original model tends to underestimate annual evapotranspiration. In the modified model, the ratio of actual to potential evapotranspiration is assumed to be a nonlinear function of both s_u and the *dryness index*, R (ratio of annual potential evapotranspiration to annual precipitation), as shown in Fig. 2(a). By allowing actual evapotranspiration to also depend on the dryness index, R, we are implicitly allowing for possible modifications of actual evapotranspiration through adaptations of natural vegetation to the environmental conditions. The increase of ET/PET with s_u expresses the increase of available water for evapotranspiration. The decrease of ET/PET with R corresponds to the restraint on ET due to the restraint of transpiration from vegetation adapted to the arid environment as well as the desiccated ground surface far from the water table under arid climate. The functional form, including the exponents R^{-5}, was chosen to mimic the Budyko curve and as yet there is no physical or causal explanation for its use.

Table 1 Meaning, values and the ranges of model parameters used in the numerical experiments

Group	Name	Description (unit)		Value and the range
Climate	P_a	Annual precipitation (mm)		1000
	R	Dryness index		0.5 (0.0—2.0)
	PET_a	Potential evapotranspiration (mm)		$P_a \cdot R$
	τ_a	Time length of one year (min)		525,600
	N_p	Meteorological period number		60
	t_m	Meteorological period (min)		$\tau_a/N_p = t_r + t_b = 8760$
	t_r	Precipitation term in a meteorological period (min)		$t_m - t_b = t_b/T = 1752$
	t_b	Non-precipitation term in a meteorological period (min)		$t_m - t_r = t_r \cdot T = 7008$
	T	Storminess index (t_b/t_r)		5.0
	P	Precipitation intensity during precipitation term (mm/min)		—
	PET	Potential evapotranspiration (mm/min)		—
	$\overline{P}$	Average precipitation intensity during precipitation term (mm/min)		$P_a/(N_P \cdot t_r)$
	$\overline{PET}$	Average potential evapotranspiration (mm/min)		PET_a/τ_a
	δ_E	(Amplitude of precipitation fluctuation)/ (average precipitation intensity)		0.0—1.0
	δ_{PET}	(Amplitude of potential evapotranspiration fluctuation)/ (average precipitation intensity)		0.0—1.0
	ω_P	Angular velocity of seasonal precipitation		$2\pi/\tau_a$
	ω_{PET}	Angular velocity of seasonal potential evapotranspiration		$2\pi/\tau_a$
	α_P	Phase difference from a standard time		0
	α_{PET}	Phase difference from a standard time		$0 \sim 2\pi$
Geographic	Z	Depth of soil layer (m)		5—20
	z_r	Average elevation of channel bed from datum (m)		1.0—16.0
	z_s	Average elevation of the bottom end of REW from datum (m)		0
	y_s	Average thickness of saturated zone (m)		$Z - y_u\ \omega_u$,0.5 Z (ini.)
	y_u	Average thickness of unsaturated zone (m)		$(Z - y_s)/\omega_u$
	ω_u	Unsaturated surface area fraction of unsaturated zone		$(Z - y_s)/y_u$
	ω_o	Saturated surface area fraction of unsaturated zone		$1 - \omega_u$
	ω_s	Horizontal area fraction of saturated zone		1
	s_u	Saturation degree of unsaturated zone		0.5 (ini.)
	Λ_u	Typical length scale for infiltration		$s_u y_u$
	Λ_s	Typical length scale for seepage outflow (m)		10
	γ_o	Slope gradient of the overland flow plane, which is assumed to be nearly flat		0.0
	L_h	Representative hillslope length of a REW in Fig. 1 (m)		500
	L_c	Total length of the channels in a REW (km)		1
	A	Area of a REW (km^2)		1
	D_d	Drainage density (1/km)		1
	D_a	Drainability index		—
	G	Slope gradient of a REW		—
Soil	K	Hydraulic conductivity (m/s)		—
	K_s	Saturated hydraulic conductivity (m/s) (*1)	Silty loam	3.4×10^{-5}
			Sandy loam	3.4×10^{-5}
			Sand	8.6×10^{-5}
	λ	Pore-disconnectedness index (*1)	Silty loam	4.7
			Sandy loam	3.6
			Sand	3.4
	ε	Porosity (*1)	Silty loam	0.35
			Sandy loam	0.25
			Sand	0.20
	m	Dimensionless parameter related to the width of the pore radius distribution (*2)	Silty loam	0.44
			Sandy loam	0.70
			Sand	0.77
	ψ_c	Bubbling pressure (m) (*2)	Silty loam	−0.20
			Sandy loam	−0.10
			Sand	−0.10
	ψ_0	Capillary pressure at the inflection point on the $\theta - \psi$ curve (m) (*2)	Silty loam	−0.30
			Sandy loam	−0.25
			Sand	−0.16

Table 1 (*continued*)

Group	Name	Description (unit)	Value and the range
	ψ_u	pressure head in the unsaturated zone	–
	v_u	Velocity in the unsaturated zone (m/s), positive when directed upward	–
	W	Storage capacity index	–
Others	ρ	Water density (kg/m^3)	1000
	g	Gravitational acceleration (m/s^2)	9.80
	t	Time	–

'*1' indicates the data are from Bras (1990), and '*2' indicates the data are obtained by the calibrations in our research. The calibration manually adjusted the parameters in Kosugi's water retention curve model, VK model (Kosugi, 1994), to fit the curves by VK model with those obtained by the Brooks–Corey equation (Brooks and Corey, 1966) and the parameters in Bras (1990) as much as possible. The ''ini.'' indicates initial condition.

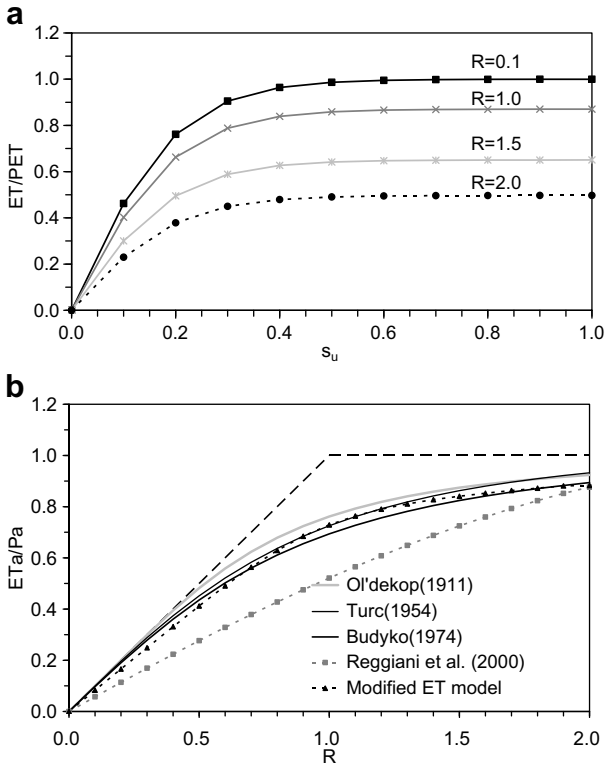

Figure 2 Modified evapotranspiration model. (a) Normalized evapotranspiration as a function of saturation degree in the unsaturated zone s_u for different dryness indices. (b) Comparison of water balance predictions with those by four other models. 'ET_a' and 'P_a' are annual evapotranspiration and annual precipitation, respectively. 'R' is dryness index, ratio of annual potential evapotranspiration over annual precipitation. 'Modified ET model' shows predictions with our modified evapotranspiration model, where soil type, soil depth, gradient, and storminess are silty loam, 8 m, 0.008, and 5.0, respectively.

With the inclusion of this revised model of evapotranspiration, the coupled water balance model produces estimates of annual actual evapotranspiration comparable to the Budyko curve (and other related empirical estimates), as shown in Fig. 2(b). Since our main concern is to explore the effects of seasonality of climate on monthly water balances, it was important that the model is capable of producing realistic annual water balances comparable to the empirical estimates; this was the reason for the correction to the evapotranspiration component. Note that the modified evapotranspiration model also neglects spatial variability of climatic and landscape properties, similar to Reggiani et al. (2000). There could be a variety of alternative approaches to incorporating the dependence of annual ET/PET ratio on average soil moisture content, including the use of nonlinear rather than linear functions. Likewise, the parameterizations of the runoff processes could be incorrect and thus might lead to reduced evapotranspiration.

Soil characteristic models

In addition to the above-mentioned relationships, we also need relationships for the soil's hydraulic properties or constitutive relations that will allow us to close the set of governing equations. Reggiani et al. (2000) used the Brooks–Corey model (Brooks and Corey, 1966) for the water retention curve, but in this paper we adopted the VK model (Kosugi, 1994). The VK model (Kosugi, 1994) is an improved three parameter model of water retention data and has the advantage that it removes the discontinuity near saturation that is present in the Brooks–Corey formulation. Eqs. (6) and (7) below are the functional forms of the VK model:

$$\psi_u = \begin{cases} \psi_c - (\psi_c - \psi_0) \cdot \left\{ \frac{(s_u)^{-1/m} - 1.0}{m} \right\}^{1.0-m} & (s_u < 1.0) \\ \psi_c & (s_u = 1.0) \end{cases} \quad (6)$$

$$s_u = \begin{cases} 1 \Big/ \left\{ 1 + m \left(\frac{\psi_c - \psi_u}{\psi_c - \psi_0} \right)^{1/(1-m)} \right\}^m & (\psi_u < \psi_c) \\ 1.0 & (\psi_u \geqslant \psi_c) \end{cases} \quad (7)$$

where ψ_c and ψ_0 are, respectively, the bubbling pressure and capillary pressure at the inflection point on the $s_u - \psi_u$ curve, and m is a parameter. For the relationship between unsaturated hydraulic conductivity K and saturation degree, we used the same Brutsaert's model (Brutsaert, 1966) as in Reggiani et al. (2000) (see in Eq. (8) below)

$$K = K_s \cdot (s_u)^{\lambda} \quad (8)$$

where λ is pore-disconnectedness index.

Numerical solution of governing equations and estimation of water balance

To solve the governing equations, it is necessary to provide initial conditions for the saturation degree in the unsaturated zone s_u and the water depth of the saturated zone y_s, soil properties, climatic inputs, and two geometric parameters γ_0 and Λ_s. We specified an initial value of 0.5 for s_u and 0.5Z for y_s, for all the numerical experiments. Parameters related to soil hydraulic properties were taken from the literature (Bras, 1990). As in Reggiani et al. (2000), the two geometric parameters of γ_0 and Λ_s were taken to be 0.0 and 10 m. For reference, all the parameter values or the ranges of parameter values used are summarized in Table 1.

In this paper we utilized the fourth-order Runge–Kutta integration method for solving the governing equations simultaneously for a single REW. Firstly, we gave the initial condition for s_u and y_s to solve Eq. (2) for ψ_u. Secondly, we solved Eqs. (1) and (3) to obtain s_u and y_s in the next step of the Runge–Kutta integration method with a time step of 5 min. Iteration under cyclic climatic inputs continues until an equilibrium condition is achieved at the annual scale. We judge the simulations to have achieved the equilibrium condition on an annual basis when the differences in estimated values of s_u and y_s between the two final days both become less than 0.00001 ($s_u$is dimensionless, y_s is in meters) for two successive years, and visually confirm it with predicted temporal variations of s_u and y_s.

Climate seasonality and annual water balance

Climatic inputs and introduction of seasonality

Neglecting inter-annual fluctuation of precipitation as well as randomness in precipitation rate, duration and arrival, we generated seasonally-varying climatic inputs by the following procedure. The first step is to estimate the average annual potential evapotranspiration intensity $\overline{PET}$ (mm/min) from the product of annual total precipitation P_a fixed at 1000 (mm/y) and the assumed dryness index R and divided by the period of one year (converted to minutes). The second step, also used by Reggiani et al. (2000), is to divide one year (=525,600 min) into N_p (=60) equally long meteorological event cycles of period, t_m (min). Each meteorological event cycle consists of a storm or event duration, t_r (min) during which precipitation is assumed to fall, and the inter-storm period, $t_b(=t_m - t_r)$ (min) which represents a break in the precipitation during which evapotranspiration and drainage are assumed to occur. The ratio of these two durations,t_b/t_r, is defined as the *storminess index*, T. The selection of N_p will clearly have some effect on our results; however, exploration of these effects is beyond the scope of this study. The third step is to evaluate the average precipitation intensity $\overline{P}$ over the rainy periods only (mm/min) by dividing annual precipitation total, P_a (mm), by the total length of rainy periods, $N_p \cdot t_r$ (min). The final step is to introduce seasonality into $\overline{P}$ (mm/min) and $\overline{PET}$ (mm/min) using Eqs. (9) and (10) given below, similar to what was done by Milly (1994a,b) and Potter et al. (2005)

$$P(t) = \begin{cases} \overline{P}\{1 + \delta_P \sin(\omega_P t + \alpha_P)\} & \text{(During storm periods)} \\ 0 & \text{(During inter-storm periods)} \end{cases}, \quad 0 \leqslant \delta_P \leqslant 1 \tag{9}$$

$$\mathrm{PET}(t) = \begin{cases} 0 & \text{(During storm periods)} \\ \overline{\mathrm{PET}}\{1 + \delta_{\mathrm{PET}} \sin(\omega_{\mathrm{PET}} t + \alpha_{\mathrm{PET}})\} & \text{(During inter-storm periods)} \end{cases}, \quad 0 \leqslant \delta_{\mathrm{PET}} \leqslant 1 \tag{10}$$

In the following simulations, α_P, ω_P, and ω_{PET} were set at 0, $2\pi/\tau_a$, and $2\pi/\tau_a$, respectively. The parameter τ_a was 525, 600 min to represent the entire annual cycle of precipitation and evapotranspiration.

Note that for simplicity seasonal variabilities of storm duration and inter-storm period, as well as other climatic variabilities, are all ignored in this study. Again, as a first step, the random variabilities of precipitation and potential evapotranspiration are ignored in this study. Finally, the neglect of fine-scale and random rainfall intensity variations means that the model is unlikely to generate infiltration excess runoff. These are some of many simplifications adopted to enable us to concentrate solely on the effects of climate seasonality on annual and monthly water balances.

Outline of numerical experiments

We carried out a series of numerical experiments to illustrate the effect of climate seasonality under different combinations of climatic dryness, soil type and depth, and topography on annual water balance. The results of the numerical experiments indicated that the effects of climate seasonality on annual water balance are as follows: (1) in general seasonality of climate leads to a reduction of annual evapotranspiration, which is likely due to the fact that stronger seasonality most likely leads to an increased range of soil moisture storage. Since runoff and actual evapotranspiration are both nonlinear functions of soil water storage, the increased range in storage produces more runoff when the soil is very wet, and less evapotranspiration when the soil is very dry; (2) these effects become most significant when $\delta_P = \delta_{\mathrm{PET}} = 1$; (3) the seasonality effects are small when $\alpha_{\mathrm{PET}} - \alpha_P$ is 0 (in-phase), and they are large when $\alpha_{\mathrm{PET}} - \alpha_P$ is π (perfectly out of phase). Hence, in the remainder of the simulations we focus on three different scenarios of climatic seasonality, which together encompass a broad spectrum of climate seasonality effects on annual water balance. The first scenario is no seasonality at all, meaning $_P = \delta_{\mathrm{PET}} = 0$ and the seasonality index $SI = |\delta_P - \delta_{\mathrm{PET}} R| = 0$ (Milly, 1994b). The second scenario is in-phase seasonality, which means $\alpha_{\mathrm{PET}} - \alpha_P = 0$ and $SI = |\delta_P - \delta_{\mathrm{PET}} R|$. The last scenario is where seasonal variabilities of precipitation and potential evapotranspiration are completely out of phase, i.e., $\alpha_{\mathrm{PET}} - \alpha_P = \pi$ and $SI = |\delta_P + \delta_{\mathrm{PET}} R|$. For brevity, the results reported in this paper are for these three conditions only, with $\delta_P = \delta_{\mathrm{PET}} = 1$ assumed for both in-phase ($SI = |\ 1 - R|$) and out-of-phase ($SI = |1 + R|$) seasonality.

Effects of climate seasonality and soil types

Fig. 3 shows the effect of seasonality on annual water balance for two different soil types and different climatic dryness values, where G is topographic gradient defined as below

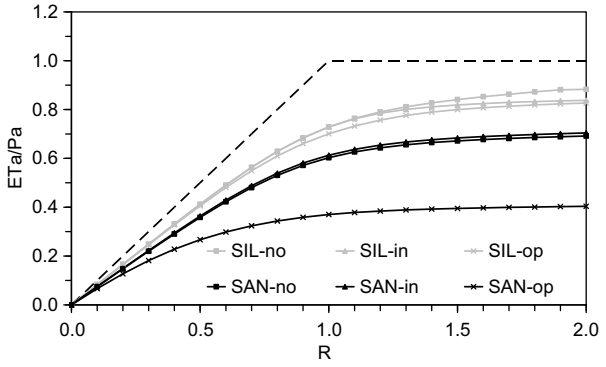

Figure 3 Effect of soil type on annual water balance: SIL and SAN refer to silty loam and sand, respectively. 'no' indicates no seasonality, 'in' indicates precipitation and potential evapotranspiration are in phase, 'op' indicates precipitation and potential evapotranspiration are of opposite phase. 'ET_a' and 'P_a' are annual evapotranspiration and annual precipitation, respectively. 'R' is dryness index, the ratio of annual potential evapotranspiration over annual precipitation. Gradient, storminess, and soil depth used in these predictions are 0.008, 5.0, 8.0 m, respectively.

$$G = \frac{Z - (z_r - z_s)}{L_h} \tag{11}$$

where z_r and z_s are elevations of channel bed and the bottom end of the representative elementary watershed (REW) from the datum, Z is depth of soil layer (m), L_h is the representative hillslope length of in a typical REW (see Fig. 1 for definition of these variables). Higher topographic gradient means, as the name implies, that the basin is steeper. Similar to the results in Reggiani et al. (2000), in our study we found that annual evapotranspiration is generally higher for more fine grained soils, decreasing as one went from silty loam to sand. The effects of seasonality can be measured in terms of the difference in annual evapotranspiration between in phase and out of phase seasonality, i.e., the width of that separates the effects of these two types of seasonality. Fig. 3 shows that, for the combination of parameters considered (i.e. relatively steep topography, $G = 0.008$), the effect of climate seasonality on annual water balance is most dominant for sand, and less (almost negligible) for silty loam. In all soils, these differences and hence the effects of seasonality increase with increasing dryness index.

To a large extent, these results can be explained based on physical considerations. Silty loam has high porosity and low hydraulic conductivity, and hence much water can be stored in the soil, meaning a higher temporal average of s_u and y_s and hence annual evapotranspiration is higher, regardless of the type of climate seasonality. On the other hand, sand has low porosity and high hydraulic conductivity, and so less water can be stored in the soil, and so more is drained through subsurface flow. This feature tends to produce lower temporal average of s_u and y_s, and hence annual evapotranspiration can be expected to be lower and subsurface runoff is higher. This effect will be considerably enhanced when the seasonal variabilities of precipitation and potential evapotranspiration are out of phase. The excess of precipitation over evapotranspiration in the wet season, along with the high permeability of sandy soils, contributes (nonlinearly) to larger amounts of subsurface runoff, and thus smaller amounts of soil moisture storage to be depleted over the dry season, leading to lower s_u and y_s values, and a significant reduction of annual evapotranspiration. On the other hand, in the case of silty loam, due to much reduced drainage, the water remains in the soil only to be evaporated again during the dry periods (when potential evaporation is higher than precipitation). This explains the much reduced effect of seasonality. In fact, as we shall see later, this is a limited explanation, and more complex behavior is manifested when the topography is flatter.

Effects of climate seasonality and topographic gradient

A basin can be deemed well drained either through highly permeable soils, or steep topography, or both. In order to investigate the effects of topographic slope, we repeated the previous simulations (reported in Fig. 3) for different values of the topographic gradient G while keeping soil depth Z constant (=8 m).

Fig. 4 shows the effects of seasonality on annual water balance for two different values of the topographic gradient and different values of climatic dryness index, with the results being reported separately for silty loam (Fig. 4a) and sand (Fig. 4b). For a high value of the gradient, $G = 0.010$ (i.e. steep topography) the results are nearly identical to what was reported in Fig. 3 for both silty loam and sand. On the other hand, when $G = 0.002$ (i.e. flat topography) the effect of seasonality appears to become more significant, especially for silty loam (Fig. 4a). Fig. 4 also shows that the annual evapotranspiration does not change significantly with change of gradient, for both types of soil, if precipitation and potential evapotranspiration have no seasonality or if their seasonal variabilities are in phase.

The results presented in Fig. 4 may appear counter-intuitive because decreasing gradient would lead to a reduction of drainability as in Bertoldi et al. (2006), and Fig. 4(a) is counter to what is reported in Fig. 3 where the effect of seasonality is less for silty loam. The explanation for this behavior is that the combination of silty loam and flat topography leads to such a drastic reduction of drainability that the water table rises to a high enough level during the wet season and produces much higher moisture content in the unsaturated zone and also saturation area extent, and hence leads to much larger amounts of surface runoff. Subsurface runoff is actually very much reduced as a result. Therefore, the difference between the effect of in-phase and out-of-phase seasonality in this instance (for silty loam) is due to a switch in the dominant runoff producing mechanism with the reduction of drainability (due to the combination of low permeability and flat topography). In the case of sand, as shown in Fig. 4(b), the watershed becomes more sensitive to climate because of the high hydraulic conductivity, making climate seasonality to become more dominant. Fig. 4 (b) also shows that flatter basins are highly sensitive to seasonality, which is the same tendency that is presented in Fig. 4(a). More insights into these interpretations can be gained by looking at the intra-annual water

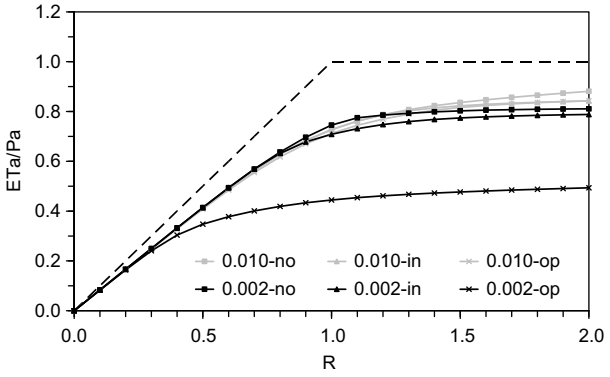

(a) silty loam

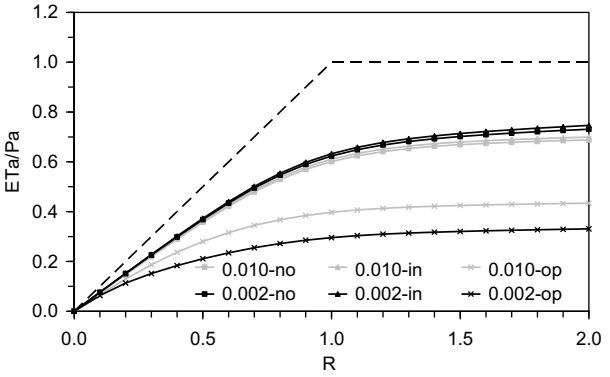

(b) sand

Figure 4 Effect of topographic gradient on annual water balance: (a) Case of silty loam, (b) Case of sand. 0.010 and 0.002 refer to topographic gradients of 0.010 and 0.002, respectively. 'no' indicates no seasonality, 'in' indicates precipitation and potential evapotranspiration are in phase, 'op' indicates precipitation and potential evapotranspiration are of opposite phase. 'ET_a' and 'P_a' are annual evapotranspiration and annual precipitation, respectively. 'R' is dryness index, the ratio of annual potential evapotranspiration over annual precipitation. Storminess and soil depth used in these predictions are 5.0, and 8.0 m, respectively.

balance dynamics, and internal processes and mechanisms, which are reported in Section 4.

Summary and discussion of annual water balance

The results presented so far demonstrate that climate seasonality, in general, has a tendency to decrease annual evapotranspiration and increase total runoff (see Figs. 3 and 4) if precipitation and potential evapotranspiration are *out of phase*, compared to the case when they are *in phase* or they have no seasonality. The effects of seasonality are greater for well drained soils (sandy soils combined with any topographic slope), in which case the reduction of annual evapotranspiration is compensated for by an increase in subsurface runoff or drainage. Interestingly, the same result happens also in case of poorly drained soils (silty loam and flat topography), but in this case this phenomenon is due to the dominance of surface runoff caused by higher water table levels in relation to the soil depth. Thus, there would appear to be some critical value of drainability and/or soil depth at which the dominant runoff process switches from subsurface to surface runoff. In general, soil type, in terms of water holding capacity and permeability, has a significant role in the type of water balance that develops in response to climate and topographic slope.

The effects of climatic seasonality on annual water balance presented so far agree qualitatively with the results of Milly (1994b). Milly (1994b) explored the effect of a storage capacity index, a product of soil porosity and soil depth, on annual evapotranspiration, finding that annual evapotranspiration increases with the increase of the storage capacity index. However, Milly did not discuss the effects of soil type itself. In addition, the use of the physically-based model in our study and the ability to switch between surface and subsurface runoff as dominant processes has allowed for a richer and more insightful exploration of the effects of seasonality.

Our results on the effects of soil type on annual evapotranspiration differ somewhat from the predictions of Eagleson (1978b) who neglected climate seasonality in his model. Our model predicted, in the case of relatively steep topography, that annual evapotranspiration was higher for fine grained soils, and less for coarse grained soils: for example, silty loam produced higher evapotranspiration and sandy soils less, but Eagleson (1978b) predicted results in the opposite order. Although there is some possibility that this difference might have been caused by the absence of climate seasonality in Eagleson (1978b), one of the possible reasons for the difference must be due to the inclusion of shallow subsurface flow in our model. The presence of coarse grained soils combined with steep hillslopes contributes to drainage of much of the precipitation that infiltrates into the soil, making it unavailable for evapotranspiration. On the other hand, in the case of flat topography and fine grained soils such as silty loam, our model predicted that the dominant runoff process could switch to surface runoff, contributing to a reduction of evapotranspiration, conforming to Eagleson's predictions. Effect of soil type on both annual evapotranspiration and surface runoff in relation to the effect of mean soil depth to water table under semi-humid climate has been explored by Salvucci and Entekhabi (1995), who included lateral hillslope processes in their water balance model. Their results showed that fine grained soils generate more evapotranspiration and surface runoff than coarse grained soils, which also supports our results. It is clear then that the competition between shallow subsurface flow, surface runoff and evapotranspiration does make both qualitative and quantitative differences to the overall water balance, and its inclusion in our model, along with the ability to analyze the underlying climatic and landscape controls, puts it at a considerable advantage vis a vis the models of Milly (1994b) and Eagleson (1978b). This competition between shallow subsurface flow, surface runoff and evapotranspiration must be mediated by the position of water table, which itself is related to topography, as explained by Salvucci and Entekhabi (1995).

Effect of climate seasonality on intra-annual water balance

Climatic seasonality affects not only annual water balance but also intra-annual (i.e. within-year) variability of water

balance behavior, e.g., the intra-annual variation of hydrological variables such as saturation degree and saturated water depth. Intra-annual variabilities and the effects of seasonal variability of climate have not received as much attention as annual water balance, and yet as we have already alluded to, they can give us valuable insights into observed (as well as predicted) water balance behavior at both the annual and seasonal time scales. In this section we explore these issues using the physically-based water balance model presented earlier. In addition to dryness index, R, we introduce a storage capacity index W (Milly, 1994a), and a drainability index, D_a, to aid in our investigation. The storage capacity index, W, and the drainability index, D_a, are defined as

$$W = \frac{\varepsilon(Z + z_r - z_s)}{2\overline{P}\tau_a} \tag{12}$$

$$D_a = \frac{K_s}{\overline{P}}\frac{Z - z_r + z_s}{L_h} = \frac{K_s}{\overline{P}}G = \frac{2K_s(Z - z_r + z_s)D_d}{\overline{P}}$$

$$\left(\text{Here we assumed } D_d = \frac{L_c}{A} = \frac{L_c}{L_c \cdot 2L_h} = \frac{1}{2L_h}\right) \tag{13}$$

where ε is the porosity of the soil, Z the depth of soil layer (m), τ_a the length of one year (min), K_s saturated hydraulic conductivity of the soil (m/s), z_r the elevation of the channel bed from the datum (m), z_s the elevation of bedrock or impermeable stratum above the datum (m), D_d the drainage density (1/km), $\overline{P}$ the average intensity of precipitation during precipitation over one year (m/min), L_c the total length of all the channel in a REW (km). The storage capacity index includes both soil type (through porosity ε) and soil depth, while the drainability index captures soil type (through K_s) and topography. The drainability index D_a could take different forms, dynamically adjusted for shorter time scale processes as in Woods (2003), but we created it as a static drainage index to characterize or classify a watershed using limited hydrological information.

Using these indices allows us to systematically explore how intra-annual variability of climate affects the monthly water balance and intra-annual variations of various hydrological quantities in different environments. In our presentation, the effects of climatic seasonality are expressed in terms of fluctuations of the saturation degree in the unsaturated zone, as well as in the saturated water depth, surface runoff, subsurface runoff, the sum of surface and subsurface runoff, and storage. The following results summarize the relationships between the intra-annual fluctuations and the above-mentioned non-dimensional parameters, namely, the dryness index, R, the storage capacity index, W, and the drainability index, D_a.

Effect of seasonality for different values of dryness index R

Fig. 5 shows the effects of climatic dryness index on monthly water balances and key internal variables under seasonally-varying climate; in this case the results are only presented for silty loam. In relation to dryness index, panels (a), (b), (c), (d), (e), and (f) present the seasonal fluctuations (i.e., maximum−minimum) of the saturation degree in the unsaturated zone, relative water table depth (relative to soil depth Z), monthly evapotranspiration ratio, monthly surface runoff ratio, monthly subsurface runoff ratio, and monthly total runoff (surface + subsurface) ratio, respectively. Monthly surface runoff (denoted by S), subsurface runoff (denoted by SS), total runoff (denoted by $S + SS$) and evapotranspiration (denoted by ET) are all normalized by the annual precipitation of 1000 mm. In each case we present results for both *in phase* seasonality (thick bands) and *out of phase* seasonality (thin bands). In addition, panel (g) and panel (h) present examples of computed monthly runoff hydrographs, as well as the surface runoff and subsurface runoff components when precipitation and potential evapotranspiration are *in phase* and *out of phase*, respectively. These last results are shown for two different values of the dryness index, R (0.1 and 2.0). For both kinds of seasonality, the mean values (taken to be the mid-points of the vertical bands) of all the variables except monthly evapotranspiration decrease monotonically with the increase of the dryness index, reflecting the drying of the soils, which also explains the corresponding increase of evapotranspiration shown in panel (c).

The thick bands in panels (a), (b), (c), (d), (e), and (f) show that the amplitudes of seasonal fluctuations of all the hydrological variables, except evapotranspiration, decrease with increasing dryness index when precipitation and potential evapotranspiration are *in phase*. This suggests in this case that as the dryness index increases much of the seasonal fluctuation in precipitation is transferred to and is balanced by the accompanying evapotranspiration: since both precipitation and evapotranspiration are in phase, soil moisture accumulation is minimized especially with increasing dryness index. On the other hand, the thin bands exhibit the corresponding seasonal fluctuations when precipitation and potential evapotranspiration are *out of phase*. In this case there is a clear distinction between wet and dry seasons, causing strong seasonality in many hydrological variables. Panel (a) demonstrates this well in terms of wide intra-annual fluctuations of mean monthly saturation degree, which increases with increasing dryness index, R. The results presented in panels (a) and (b) show that the storage in the unsaturated zone absorbs much of the seasonal climatic fluctuations, which is eventually taken up by evapotranspiration. This can be seen by the amplitudes of seasonal fluctuations of relative saturated zone thickness shown in panel (b), which are relatively smaller than those of the degree of saturation shown in panel (a), and indeed decrease with increasing dryness index. Out of phase seasonality does cause wider seasonal fluctuations of subsurface and total runoff, as compared to when precipitation and potential evapotranspiration are in phase, and the fluctuations, in all cases decrease with increasing dryness index, as can be seen in panels (e) and (f). The decreases of both mean runoff and the amplitude of its seasonal fluctuations with increasing dryness index are once again due to the increase of evapotranspiration. On the other hand, it is interesting that the differences between in phase and out of phase seasonality are small to negligible in humid climates ($R < 0.5$) and become larger with increasing dryness index, R, allowing us to conclude that the effects of climatic seasonality in general become stronger with increasing aridity.

Panels (g) and (h) show, as already alluded to, that the intra-annual variations of total runoff, as well as its compo-

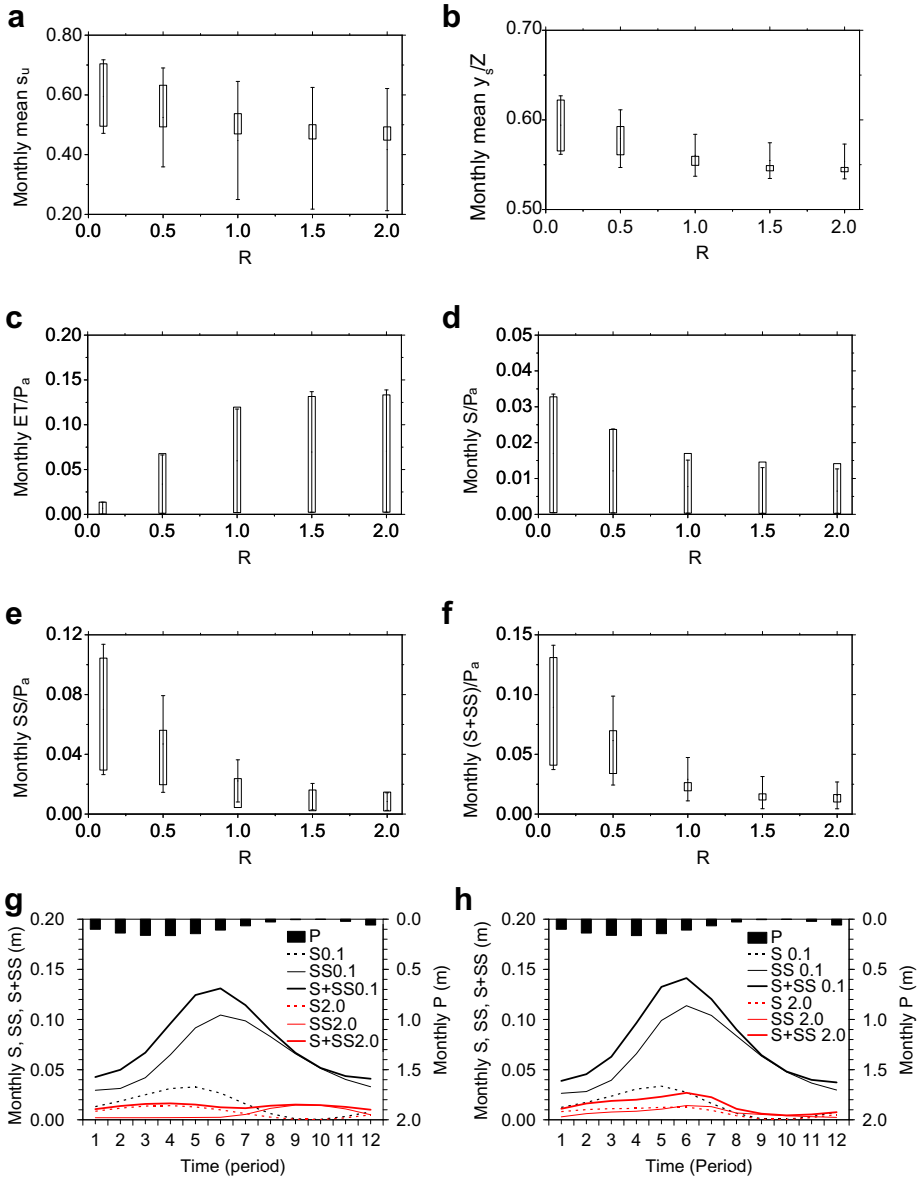

Figure 5 Effect of dryness index R and climate seasonality on (a) monthly mean saturation degree s_u, (b) monthly mean relative saturated water depth y_s/Z, (c) monthly evapotranspiration ratio ET, (d) monthly surface runoff ratio S, (e) monthly subsurface runoff ratio SS, (f) monthly total runoff ratio $S + SS$, (g) monthly hydrographs (in phase), (h) monthly hydrographs (opposite phase). The thick bands indicate fluctuation widths when precipitation and potential evaporation are in phase, and the thin bands indicate fluctuation widths when they are of opposite phase. In panels (g) and (h), numbers after S, SS, and $S + SS$ are the dryness indices. P, R, P_a, and Z are precipitation, dryness index, annual precipitation, and soil depth, respectively. Soil type, gradient, storminess index, and soil depth used in the predictions are silty loam, 0.008, 5, and 8 m, respectively. Soil depth below river bed $z_r - z_s$ is set at 4.0 m, making it a steep topography favouring strong subsurface runoff dominance.

nents, appear more uniform when precipitation and potential evapotranspiration are *in phase* than when they are *out of phase*. The difference between in phase and out of phase seasonality is, as expected, small in humid catchments ($R = 0.1$), and becomes stronger as the dryness index increases (e.g., $R = 2$). When precipitation and potential evapotranspiration are in phase they generate less instantaneous storage within the catchment, which tends to reduce the potential for both surface and subsurface runoff. On the other hand, when they are out of phase they tend to generate more instantaneous soil moisture storage, which contributes to an increase of both surface and subsurface runoff due to the nonlinear dependence of these runoff components on subsurface storage. From these results we can conclude that the effects of climatic seasonality become most dominant in arid climates when precipitation and potential evapotranspiration are out of phase.

Effect of seasonality for different values of the storage capacity index W

Fig. 6 shows the effects of changing storage capacity index as well as soil type on monthly water balance, and the

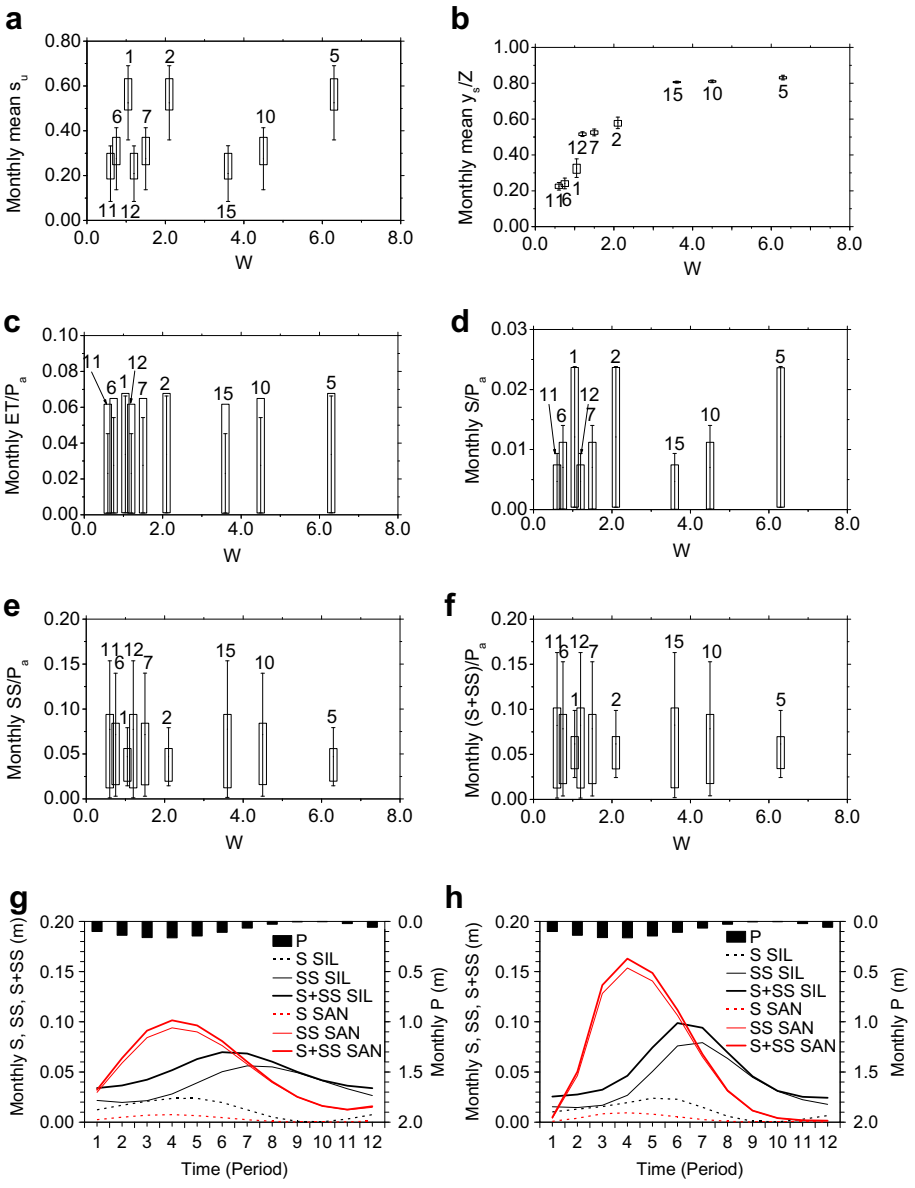

Figure 6 Effect of storage capacity index W, soil type and climate seasonality on (a) monthly mean saturation degree s_u, (b) monthly mean relative saturated water depth y_s/Z, (c) monthly evapotranspiration ratio ET, (d) monthly surface runoff ratio S, (e) monthly subsurface runoff ratio SS, (f) monthly total runoff ratio $S + SS$, (g) monthly hydrographs (in phase), (h) monthly hydrographs (opposite phase). Markers 1, 2, and 5 indicate silty loam, 6, 7, and 10: sandy loam, 11, 12, and 15: sand. Markers 1,6,11 indicate 5 m soil depth, 2, 7, 12: 8 m soil depth, 5, 10, 15: 20 m soil depth. The thick bands indicate fluctuation widths when precipitation and potential evaporation are in phase, and the thin bands indicate fluctuation widths when they are of opposite phase. In panel (g) and (h), SIL and SAN after S, SS, and $S + SS$ indicate silty loam and sand, respectively. P and P_a are monthly precipitation and annual precipitation, respectively. Gradient, storminess index, and dryness index used in these predictions are 0.008, 5, and 0.5, respectively. Soil depth below channel bed z_r—z_s had no effect at all on the results, and only soil type was changed in the panel (g) and (h). Note that data number 3, 4, 8, 9, 13, and 14 are missing in the panels (a) to (f).

intra-annual variation of the same key hydrological variables as presented in Fig. 5, under seasonally-varying climate. In Fig. 6, we varied soil depth Z by varying z_r—z_s, all the while keeping G constant (=0.008, i.e., relatively steep, causing subsurface runoff dominance); hence drainability remains constant for a given soil, and varies with only a change of soil type. In other words, in Fig. 6 we show the effect of z_r—z_s. Here we changed soil depth from 5 m to 20 m, while keeping $Z - (z_r - z_s)$ at 4.0 m.

The results obtained are rather complex and subtle and require careful interpretation. Firstly, water balance is found to be strongly dependent on the soil type regardless of storage capacity index. As expected, the degree of saturation within the unsaturated zone is higher for fine grained soils such as silty loam than for coarse grained soils such as sand, as seen in panel (a). Indeed, within each soil type keeping D_a constant, we find that both the mean and the amplitude of fluctuations of key hydrological variables do not

change with change of soil storage capacity W, which is closely tied to soil depth. The exception is the saturation zone thickness, which as seen in panel (b), increases with W for each soil type, although the growth of y_s/Z slows down with increases of W, which is directly linked to the increase of $z_r - z_s$. In general, the amplitudes of the seasonal fluctuations shown in panels (a), (e), and (f) are larger when the seasonal variabilities precipitation and potential evapotranspiration are out of phase than when they are in phase. In relation to the effects of soil type, the seasonal fluctuations of surface runoff are higher for fine grained soils (e.g., silty loam) than for coarse grained soils (e.g., sand), whereas the pattern is reversed for subsurface flow. This suggests that whether the seasonal fluctuations of total runoff is greater for fine grained soils or coarse grained soils depends on whether the dominant runoff generation mechanism is subsurface streamflow or surface runoff. If it is the former (i.e. subsurface), then the amplitudes of fluctuations will be higher with coarse grained soils, and vice versa. Recall that the results presented in Fig. 6 were for relatively steep topography, conditions under which subsurface flow dominates. Which mechanism dominates in any basin depends on climate, soil and

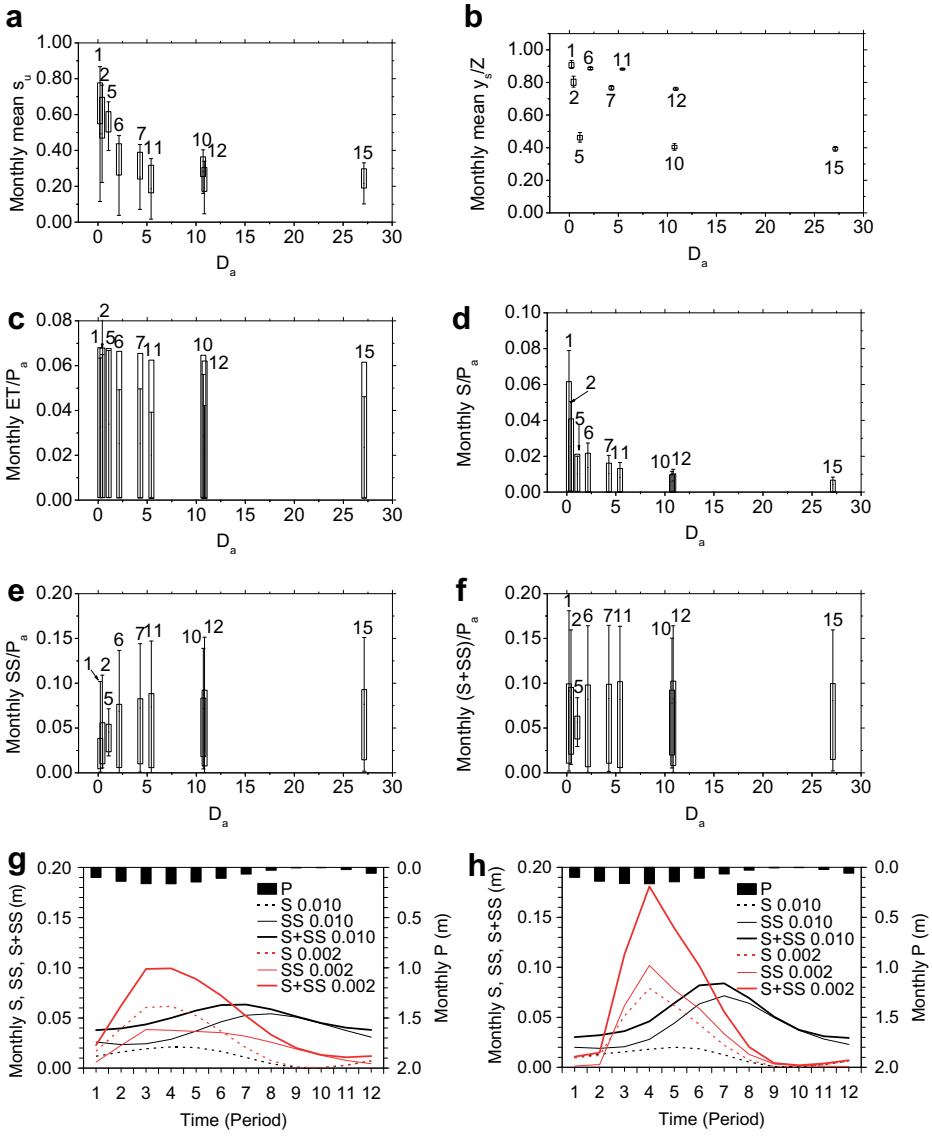

Figure 7 Effect of drainability index D_a and climate seasonality on (a) monthly mean saturation degree s_u, (b) monthly mean relative saturated water depth y_s/Z, (c) monthly evapotranspiration ratio ET, (d) monthly surface runoff ratio S, (e) monthly subsurface runoff ratio SS, (f) monthly total runoff ratio $S + SS$, (g) monthly hydrographs (in phase) for silty loam, (h) monthly hydrographs for silty loam (opposite phase). Markers 1, 2, and 5 indicate silty loam, 6, 7, and 10: sandy loam, 11, 12, and 15: sand. Markers 1, 6, 11 indicate gradient is 0.002, 2, 7, 12: 0.004, 5, 10, 15: 0.010. The thick bands indicate fluctuation widths when precipitation and potential evaporation are in phase, and the thin bands indicate fluctuation widths when they are of opposite phase. In panel (g) and (h), 0.010 and 0.002 after S, SS, and $S + SS$ indicate gradient. P, R, P_a, and Z are monthly precipitation, dryness index, annual precipitation, and soil depth, respectively. Dryness index, storminess index, and soil depth used in these predictions are 0.5, 5, 8 m, respectively. Soil depth, controlled by changing $z_r - z_s$, had no effect on the results, and only gradient had changed in the panel (g) and (h). Note that data number 3, 4, 8, 9, 13, and 14 are missing in the panels (a) to (f).

topography, requires further careful investigation, and is beyond the scope of this work.

Panel (g) and panel (h) show monthly flow hydrographs when the seasonal variations of precipitation and potential evapotranspiration are, respectively, in phase and out of phase. Since change of soil depth through the change of $z_r - z_s$ did not have any impact whatsoever on the results, (note that soil depth would have an impact if G was varied), only soil type was allowed to change between these two panels. We can see that climate seasonality becomes most effective in sandy soils when precipitation and potential evapotranspiration are out of phase, least important when the soil is silty loam and precipitation and potential evapotranspiration are in phase. This is as expected, considering that for the slope used, for both types of soils (i.e., sand and silty loam) subsurface runoff dominates and therefore the amplitudes are larger for the sand than for the silty loam. If a much flatter topography had been used, it is likely that silty loam would produce substantial surface runoff and much less subsurface runoff, a result that could impact substantially on the seasonal fluctuations of runoff. This is discussed in more detail with respect to Fig. 7 in the next section.

Effect of seasonality for different values of the drainability index D_a

Fig. 7 shows the effect of the drainability index and soil type on the water balance and the within-year fluctuations of key hydrological variables under seasonally changing climate. Here gradient G is varied while keeping soil depth Z constant at 8 m. The layout of the results is identical to that used in Figs. 5 and 6. As in Fig. 6, the results presented in Fig. 7 confirm the strong effects of soil type; the differences between soil types tend to stand out in comparison to the effects of drainability index. The thick bands in panels (a), (b), (c), (d), (e), and (f) present the amplitudes of seasonal fluctuations of several hydrological variables when precipitation and potential evapotranspiration are *in phase*. The thin bands in panels (a), (b), (c), (d), (e) and (f) show the effects of climate seasonality when precipitation and potential evapotranspiration are *out of phase*. It is clear that in almost all cases the amplitudes are larger in the case of out of phase seasonality except for evapotranspiration in panel (c).

Within each soil type, an increase of drainability (i.e. increase of gradient) leads to a reduction of the amplitude of fluctuations of seasonal variability. This is most evident in the case of silty loam, as can be seen in panels (a), (d) and (f). For the other soil types, the reduction is fairly small or negligible, and in the case of subsurface flow it shows a slight increasing trend. Panel (b) shows that an increase in drainability leads to a sharp reduction of saturation zone thickness for any given soil type.

Some of the results presented in Fig. 7 may seem counter-intuitive. Increase of drainability index, as the name implies, must mean more well-drained landscapes. Yet, in the case of silty loam, it leads to reductions in mean surface runoff and the amplitudes of the seasonal fluctuations of mean moisture content in the unsaturated zone, surface runoff, and total runoff, especially in the case of out of phase seasonality. The reductions of the mean and amplitude of total runoff in Fig. 7(f) are counter to the results presented in Fig. 6(f) where the larger fluctuations were associated with coarse grained, i.e., well-drained soils. The explanation for this apparent contradiction can be found in panels (g) and (h).

Panels (g) and (h) are runoff hydrographs for silty loam, for two different values of the gradient, i.e., $G = 0.010$ (steep slope, higher value of drainability index) and $G = 0.002$ (mild slope, smaller value of drainability index). They show that monthly runoff is most sensitive to climate seasonality if precipitation and potential evapotranspiration are out of phase and the basin is mildly sloping, $G = 0.002$. When one combines silty loam and mild slope, one obtains a poorly drained system, and yet it is this system that produces the larger amplitude of seasonal fluctuations, which contradicts our expectation and the results of Fig. 6. The explanation is by way of the composition of the runoff that is produced. In panels (g) and (h), and for $G = 0.002$, surface runoff and subsurface runoff are of almost the same magnitude, whereas for $G = 0.010$ (steep slope), the dominant runoff mechanism is subsurface runoff. In other words, a poorly drained system consisting of silty loam and small topographic slope produces larger fluctuations (compared to steep slope) of subsurface runoff also, not only surface runoff; this contradicts somewhat the interpretation that better drainage increases fluctuations of subsurface runoff. Therefore, these results suggest that a switch in dominant runoff processes may happen for some combination of soil type (fine grained soil) and gradient (mild or flat slope) at which the dominant runoff process switches from subsurface runoff only to surface runoff (or a combination of both). When this happens, the impacts of seasonality also go through a qualitative transformation: when subsurface runoff dominates, the amplitude of seasonal fluctuations is larger for well-drained systems. On the other hand, when surface runoff dominates, the amplitude of fluctuations is higher for poorly drained systems.

Summary and conclusions

The research presented in this paper has investigated the effects of climatic seasonality on annual and monthly water balances, and the role of soil and topography in modulating these impacts. The results presented in this paper were obtained using the theoretically derived physically-based water balance model of Reggiani et al. (2000), combined with a slightly modified evapotranspiration model that is dependent also on the climatic dryness index. For simplicity, the climatic seasonality was modeled by sinusoidal functions for both precipitation and potential evapotranspiration.

The results on the annual water balance are as follows: In general the presence of climatic seasonality tends to decrease evapotranspiration and increase runoff compared to when there is no seasonality, with the impacts of seasonality being the strongest when seasonal variabilities of precipitation and potential evapotranspiration are out of phase (Figs. 3 and 4). This tendency becomes stronger as the dryness index increased (e.g., semi-arid catchments).

The results obtained for annual water balance and discussed above become more clear and insightful when combined with the results of monthly water balance. So long as

subsurface runoff remains the dominant runoff generating mechanism, these effects of seasonality are higher for more well drained systems or soils than for more poorly drained systems or soils. On the other hand, for systems that are poorly drained (e.g., silty loam soils) where surface runoff dominates as a consequence, the seasonality effects manifest more strongly in flat basins than in steep basins. These results are, however, not applicable to catchments where infiltration excess runoff dominates. Owing to the fact that, in this study, rainfall intensities are averaged over event duration our model cannot simulate infiltration excess runoff generation realistically.

The effects of seasonality on monthly water balances can be summarized as follows: Intra-annual fluctuations of hydrological variables are generally enhanced when precipitation and potential evapotranspiration are out of phase compared to when they are in phase. Seasonal fluctuations are high for the combination of silty loam and mildly sloping topography (i.e., poorly drained systems) when surface and subsurface runoff both occur, or surface runoff dominates. On the other hand, seasonal fluctuations are also high for the combination of sand and steep topographic gradients (i.e., well-drained systems) in which case subsurface runoff dominates.

Indeed, there appears to be a critical combination of soil type and gradient at which a switch from subsurface to surface runoff dominance takes place. As one can very well guess, as one moves from well drained to poorly drained basins, the amplitude of the seasonal fluctuations initially decreases and at some value of the drainability index it might increase again due to the switch from subsurface to surface runoff dominance. This has implications not only for the overall water balance but also for landscape stability and vegetation establishment and survival. This requires further study, especially focused on possible co-evolution of climate, soil, vegetation and topography.

An important conclusion is that the effects of soil types are very important and very subtle. Our simulations have shown that the effects of soil type on water balance cannot be handled by means of the soil storage capacity alone, as in many conceptual bucket-type models. The role of the unsaturated zone storage, and the effects of soil permeability and their interactions with topographic slope have been shown to be important in determining both annual and seasonal water balances. These results confirm previous observations and model predictions of the critical role played by the unsaturated zone storage and time delay (Farmer et al., 2003; Struthers et al., 2006; Son and Sivapalan, 2007).

These general conclusions confirm and extend the results of the previous work done by Eagleson (1978a,b), Milly (1994a,b), Salvucci and Entekhabi (1995), Woods (2003) and Potter et al. (2005) and have provided a richer perspective of the role that interactions of climate, soil and topography play on annual and monthly water balances. The results and conclusions from this study applied only at the hillslope scale, and are potentially useful towards interpreting annual and seasonal water balances extracted from empirical observations in actual small catchments, and to compare and contrast catchments in different parts of the world on the basis of their dominant process controls. In particular, the deep insights into the climate, soil and topographic controls on annual and monthly water balances gained in this study can help formulate new approaches to catchment classification and similarity analyses. Progress in this direction can go a long way towards assisting with predicting the hydrological responses of ungauged basins.

Acknowledgements

The first author is grateful for the financial support provided by the JSPS Research Fellowship for Young Scientists and the Grant-in-Aid for JSPS fellows and a research grant from the Maeda Engineering Foundation which enabled him to spend 18 months at the University of Western Australia (UWA) and conduct the research presented in this paper. He is also grateful to the Centre for Water Research at UWA for providing the facilities to carry out much of this research. The authors also thank the Grant-in-Aid for Young Scientists (B) for the preparation of this paper. The present study is partly supported by the ''Wisdom of Water'' (Suntory) Corporate Sponsored Research Program, donated by the Suntory corporation, Japan.

References

Bertoldi, G., Rigon, R., Over, T.M., 2006. Impact of watershed geomorphic characteristics on the energy and water budgets. J. Hydromet. 7, 389–403.

Bras, R.L., 1990. Hydrology — An Introduction to Hydrologic Science. Addison-Wesley-Longman, Reading, Mass, USA.

Brooks, R.H., Corey, A.T., 1966. Properties of porous media affecting fluid flow. J. Irrig. Drain. Div. Am. Soc. Civ. Eng. IR2, 61–88.

Brutsaert, W., 1966. Probability laws for pore-size distributions. Soil Sci. 101, 85–92.

Budyko, M.I., 1974. Climate and Life. Academic Press, New York, USA.

Choudhury, B.J., 1999. Evaluation of an empirical equation for annual evaporation using field observations and results from a biophysical model. J. Hydrol. 216 (1–2), 99–110. doi:10.1016/S0022-1694(98)00293-5.

Eagleson, P.S., 1978a. Climate, soil, and vegetation, 3: A simplified model of soil moisture movement in the liquid phase. Water Resour. Res. 14, 722–730.

Eagleson, P.S., 1978b. Climate, soil, and vegetation, 6: Dynamics of the annual water balance. Water Resour. Res. 14, 749–764.

Farmer, D.L., Sivapalan, M., Jothityangkoon, C., 2003. Climate, soil and vegetation controls upon the variability of water balance in temperate and semi-arid landscapes: Downward approach to hydrological prediction. Water Resour. Res. 39 (2), 1035. doi:10.1029/2001WR000328.

Kosugi, K., 1994. Three-parameter lognormal distribution model for soil water retention. Water Resour. Res. 30, 891–901. doi:10.1029/93WR02931.

Milly, P.C.D., 1994a. Climate, interseasonal storage of soil water, and the annual water balance. Adv. Water Resour. 17, 19–24. doi:10.1016/0309-1708(94)90020-5.

Milly, P.C.D., 1994b. Climate, soil water storage, and the average annual water balance. Water Resour. Res. 30, 2143–2156. doi:10.1029/94WR00586.

Ol'dekop, E.M., 1911. On evaporation from the surface of river basins. Trans. Meteorol. Observ. Univ. Tartu 4, 200.

Pike, J.G., 1964. The estimation of annual run-off from meteorological data in a tropical climate. J. Hydrol. 2 (2), 116–123. doi:10.1016/0022-1694(64)90022-8.

Potter, N.J., Zhang, L., Milly, P.C.D., McMahon, T.A., Jakeman, A.J., 2005. Effects of rainfall seasonality and soil moisture capacity on

mean annual water balance for Australian catchments. Water Resour. Res. 41, W06007. doi:10.1029/2004WR003697.

Reggiani, P., Sivapalan, M., Hassanizadeh, S.M., 1998. A unifying framework for watershed thermodynamics: balance equations for mass, momentum, energy and entropy, and the second law of thermodynamics. Adv. Water Resour. 22 (4), 367–398. doi:10.1016/S0309-1708(98)00012-8.

Reggiani, P., Hassanizadeh, S.M., Sivapalan, M., Gray, W.G., 1999. A unifying framework for watershed thermodynamics: constitutive relationships. Adv. Water Resour. 23 (1), 15–19. doi:10.1016/S0309-1708(99)00005-6.

Reggiani, P., Sivapalan, M., Hassanizadeh, S.M., 2000. Conservation equations governing hillslope responses: Exploring the physical basis of water balance. Water Resour. Res. 36, 1845–1863. doi:10.1029/2000WR900066.

Salvucci, G.D., Entekhabi, D., 1995. Hillslope and climatic controls on hydrologic fluxes. Water Resour. Res. 31, 1725–1939.

Schreiber, P., 1904. Uber die Beziehungen zwischen dem Niederchlag und der Wasserfuhrung der Flusse in Mittelleuropa. Z. Meteorol. 21, 441–452.

Sivapalan, M. et al, 2003. IAHS Decade on Predictions in Ungauged Basins (PUB), 2003–2012: Shaping an exciting future for the hydrological sciences. Hydrol. Sci. J. 48 (6), 857–880.

Son, K., Sivapalan, M., 2007. Improving model structure and reducing parameter uncertainty in conceptual water balance models through the use of auxiliary data. Water Resour. Res. 43, W01415. doi:10.1029/2006WR005032.

Struthers, I., Hinz, C., Sivapalan, M., 2006. A multiple event gravity-based wetting front and redistribution model for water balance applications. Water Resour. Res. 42 (6), W06406. doi:10.1029/2005WR004645.

Turc, L., 1954. Le bilan d'eau des sols: Relation entre les precipitations, l'evaporation er l'ecoulement. Ann. Agron. 5, 491–569.

Woods, R.A., 2003. The relative roles of climate, soil, vegetation and topography in determining seasonal and long-term catchment dynamics. Adv. Water Resour. 26 (3), 295–309. doi:10.1016/S0309-1708(02)00164-1.

Zhang, L., Dawes, W.R., Walker, G.R., 2001. Response of mean annual evapotranspiration to vegetation changes at catchment scale. Water Resour. Res. 37 (3), 701–708, 2000WR900325.